TABLE II: Summary of N_2O_5 Cross Sections[a,b]

λ/nm	no. of runs	$10^{19}\sigma$/cm²	λ/nm	no. of runs	$10^{19}\sigma$/cm²
280	53	1.17	240	27	6.2
275	50	1.30	235	24	7.7
270	48	1.61	230	17	9.9
265	42	2.0	225	10	14.4
260	40	2.6	220	10	22
255	28	3.2	215	10	37
250	33	4.0	210	8	56
245	29	5.2	205	4	82
			200	4	92

[a] λ = 380-285 nm. T = 225-300 K. Number of runs = 660. $\ln(10^{19}\sigma/\text{cm}^2) = 0.432537 + (4.72848 - 0.0171269\lambda)(1000/T)$. [b] λ = 280-200 nm. Little or no temperature dependence, and all data at one temperature averaged together.

Although there is some hint of temperature effect on the N_2O_5 cross section below 280 nm, Figure 2, the trend is so slight that all data points from 223 to 300 K of both series one and series two were averaged every 5 nm between 200 and 280 nm, and these data are given in Table II. Below 230 nm these results are exclusively from the second series, and they are based on the kinetic method, which tends to eliminate the perturbing effect of HNO_3 on the results.

Previous measurements[1-3] of the N_2O_5 cross sections were done at 298 or 300 K. The line in Figure 4 is based on the average observed points (Table II) from 200 to 280 nm and the points calculated (25) from 285 to 380 at 300 K. The circles represent Graham's[3] values and the triangles represent the results of Jones and Wulf.[1] The present results are fairly well parallel to those of Graham between 210 and 310 nm but are about 10% higher. The present results are not strictly parallel to and average about 30% higher than those of Jones and Wulf between 290 and 380 nm. In view of the difficulty in handling N_2O_5 and its decomposition products, Figure 4 shows reasonably good agreement between these and other results at 300 K.

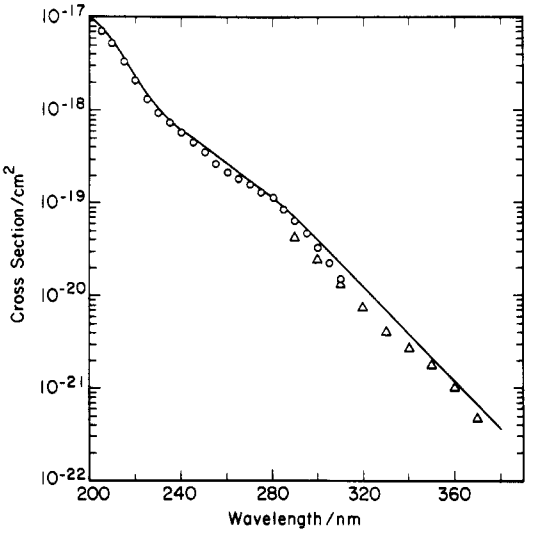

Figure 4. Comparison of N_2O_5 cross sections at 298 K as found by this study (the line) and as found by Graham and Johnston (circles) and by Jones and Wulf (triangles).

Discussion

The explanation for the increase with temperature in cross section at long wavelengths is that thermal excitation of vibrational and rotational states in the ground electronic state of the molecule makes available low-energy, long-wavelength transitions. The population of such states is expected to parallel the Boltzmann factor, $\exp(-\epsilon/kT)$, and the linear relation shown in Figure 3 is reasonable. Such an effect may be expected on the long-wavelength side of an absorption peak, but regions near the maximum of the absorption peak usually show little or no effect of modest temperature changes.

The decrease of cross section with decrease of temperature largely occurs above 300 nm. For considerations of atmospheric photochemistry, this is the wavelength region where solar radiation penetrates to the troposphere and to the ground. Thus the temperature dependence of the N_2O_5 cross section may be of some importance to the low-temperature upper troposphere and lower stratosphere.

Acknowledgment. This work was supported by the Director, Office of Energy Research, Office of Basic Energy Sciences, Chemical Sciences Division of the U.S. Department of Energy under Contract No. DE-AC03-76SF00098.

Photon Absorption: Classical Treatment of Nuclear Motion

Jack Simons†

Chemistry Department, University of Utah, Salt Lake City, Utah 84112 *(Received: March 24, 1982; In Final Form: May 14, 1982)*

In this paper, we consider, within a first-order perturbation treatment, the photon-induced electronic transition process as it appears in the quantum, classical, and partly classical points of view. Advantages and limitations of each approach are stressed, and their relevance to time-resolved and frequency-resolved experiments involving small, large, and predissociating molecules is discussed. We also show how each point of view can be used to generate coordinates and momenta which serve as initial conditions for classical trajectory studies of the fate (e.g., predissociation) of the electronically excited molecules formed in the photon absorption. The emphasis of this paper is twofold. It attempts to shed light on how the effects of photon absorption can be viewed in the classical or quantum frameworks. It also shows how the various points of view differ in their practical utility with respect to the computation of absorption intensities or the evaluation of initial coordinates and momenta for use in classical dynamics work.

I. Photon Absorption Rate

The conventional electric dipole expression for the rate of photon-induced transitions between initial and final Born–Oppenheimer (BO) states $\phi_0 X_i^0$ and $\phi_f X_v^f$, respectively, is given by[1]

$$W_{0i,fv} = \frac{2\pi}{\hbar} |\langle \phi_0 X_i^0 | \vec{\epsilon}\cdot\vec{r} | \phi_f X_v^f \rangle|^2 \, \delta[\omega - (\epsilon_v^f - \epsilon_i^0)/\hbar] \text{ s}^{-1} \quad (1)$$

†David P. Gardner Fellow; Camille and Henry Dreyfus Fellow.

0022-3654/82/2086-3615$01.25/0

Here ϵ_i^0 and ϵ_v^f are the total BO energies (electronic plus vibration/rotation) of the initial and final states, $\hbar\omega$ is the energy of the incident photon, and $\vec{\epsilon}\cdot\vec{r}$ is the electric dipole interaction potential. We have denoted by $\hbar$ Planck's constant divided by 2π. ϕ_0 and ϕ_f are the BO electronic wave functions which obey[2] $h_e\phi_0 = E_0\phi_0$ and $h_e\phi_f = E_f\phi_f$. The total Hamiltonian H consists of the electronic part h_e (containing electron kinetic energy, electron–electron and nuclear–nuclear repulsion, and electron–nucleus attraction) plus the nuclear kinetic energy operator T. The vibration–rotation eigenstates, which obey $(T + E_f)X_v^f = \epsilon_v^f X_v^f$, are functions of all of the molecule's internal and orientational degrees of freedom.

A convenient expression for the total rate of absorption of light of energy $\hbar\omega$ due to molecules initially in $\phi_0 X_i^0$ can be obtained by summing eq 1 over all final states and using the well known integral expression for the Dirac δ function: $\delta(\omega - (E/\hbar)) = (1/2\pi)\int_{-\infty}^{\infty} \exp[i(\omega - E/\hbar)t]\,dt$

$$W = \sum_{f,v} \frac{1}{\hbar} \int_{-\infty}^{\infty} \exp(i\omega t)\langle \phi_0 X_i^0 | \exp(iHt/\hbar)\vec{\epsilon}\cdot\vec{r}\exp(-iHt/\hbar)|\phi_f X_v^f\rangle\langle\phi_f X_v^f|\vec{\epsilon}\cdot\vec{r}|\phi_0 X_i^0\rangle\,dt \quad (2)$$

The $\exp(\pm iHt/\hbar)$ factors arise from $\exp(i\epsilon_i^0 t/\hbar)$ and $\exp(-i\epsilon_i^f t/\hbar)$, respectively.

To understand why this form for W is especially convenient, let us examine what happens if we now treat the nuclear motion (vibration–rotation) classically. In this case, the quantum mechanical operator T (which does not commute with h_e) is *assumed* to commute with h_e. We designate this approximation by placing the subscript c on the nuclear kinetic energy operator $T \simeq T_c$. Under this approximation, the term $\exp(iHt/\hbar)\vec{\epsilon}\cdot\vec{r}\exp(-iHt/\hbar)$ reduces to $\exp(ih_e t/\hbar)\vec{\epsilon}\cdot\vec{r}\exp(-ih_e t/\hbar)$, since T_c commutes[3] with h_e and $\vec{\epsilon}\cdot\vec{r}$. By then using the fact that ϕ_0 and ϕ_f are eigenfunctions of h_e, we can rewrite W, within this classical treatment of the nuclear kinetic energy, as

$$W_c = \sum_{f,v} \frac{1}{\hbar} \int_{-\infty}^{\infty} \exp(i\omega t)\langle \phi_0 X_i^0|\vec{\epsilon}\cdot\vec{r}\exp[it(E_0 - E_f)/\hbar] \times |\phi_f X_v^f\rangle\langle\phi_f X_v^f|\vec{\epsilon}\cdot\vec{r}|\phi_0 X_i^0\rangle\,dt \quad (3)$$

Recall that ϕ_0, ϕ_f, X_v^0, X_v^f, E_0, and E_f are all functions of the molecule's internal coordinates $\{\vec{R}\}$. Because the vibration–rotation eigenfunctions $\{X_v^f\}$ form a complete set for any state ϕ_f, we can use $\sum_v |X_v^f\rangle\langle X_v^f| = 1$ to simplify eq 3. Introducing the electronic transition dipole matrix element[4] $\mu_{0f} = \langle\phi_0|\vec{\epsilon}\cdot\vec{r}|\phi_f\rangle$, W_c can be written as

$$W_c = \sum_f \frac{1}{\hbar}\int_{-\infty}^{\infty} \exp(i\omega t)\langle X_i^0|\mu_{0f}^*\mu_{0f}\exp[it(E_0 - E_f)/\hbar]X_i^0\rangle\,dt = \sum_f \frac{2\pi}{\hbar}\langle X_i^0||\mu_{0f}|^2\,\delta[\omega - (E_f - E_0)/\hbar]|X_i^0\rangle \quad (4)$$

which represents our partly classical approximation to the photon absorption rate.

II. Comparison of Quantum and Classical Expressions

It should not be surprising that the fully quantum expression (eq 1 or 2) for W is not identical with the partly classical (the electronic degrees of freedom are still treated quantum mechanically) expression given in eq 4. However, it is fruitful to explore the similarities and differences in W and W_c. In particular, let us examine the ω dependence of each expression as well as the intensity distribution of the respective absorption rates.

A. The Classical Picture. W_c tells us that a photon of energy $\hbar\omega$ will be absorbed at molecular geometries $\{\vec{R}\}$ where $\hbar\omega = E_f(\vec{R}) - E_0(\vec{R})$. This, of course, simply states that the photon absorption causes a purely electronic transition[5] (from ϕ_0 to ϕ_f) giving rise to a change in the *electronic* energy equal to $E_f(\vec{R}) - E_0(\vec{R})$. Equation 4 shows that the intensity (value of W_c at this $\hbar\omega$) of the absorption corresponding to $\hbar\omega = E_f(\vec{R}) - E_0(\vec{R})$ is equal to $(2\pi/\hbar)|X_i^0(\vec{R})|^2|\mu_{0f}(\vec{R})|^2$. This can be interpreted as the probability density $|X_i^0|^2$ for finding the molecule at $\vec{R}$ times the rate $(2\pi/\hbar)|\mu_{0f}(\vec{R})|^2$ of the electronic transition at that $\vec{R}$ value. It follows from this interpretation of W_c that a *purely classical* treatment of vibration and rotation leads to the prediction of a "smooth" absorption spectrum whose intensity at $\hbar\omega$ is given as the integral over all molecular geometries obeying $\hbar\omega = E_f(\vec{R}) - E_0(\vec{R})$ of the intensity factor $|X_i^0|^2(2\pi/\hbar)|\mu_{0f}|^2$. For example, if $E_f(\vec{R})$ and $E_0(\vec{R})$ were one-dimensional harmonic oscillator potentials corresponding to different geometries but with identical frequencies ($E_0 = ax^2$, $E_f = \Delta + a(x - x_0)^2$) and if X_i^0 were the ground-state harmonic oscillator function of E_0, $X_i^0 = A\exp(-\alpha x^2)$, then the ω dependence of the absorption would involve $A^2\exp[-2\alpha(\hbar\omega - \Delta - ax_0^2)^2/4a^2x_0^2]$ since $\hbar\omega = E_f - E_0$ gives $x^2 = (\hbar\omega - \Delta - ax_0^2)^2/4a^2x_0^2$. If the x dependence of $|\mu_{0f}|^2$ is neglected, this would then give rise to a Gaussian absorption line shape which is the ω space image of $|X_i^0|^2$. The Gaussian is centered at $\hbar\omega = \Delta + ax_0^2$, which corresponds to the "vertical" transition occurring at the maximum of $|X_i^0|^2$ (at $x = 0$). Although this example is very simplified, it illustrates the more general relationship between the "shape" of $|X_i^0|^2$ in $\vec{R}$ space and the shape of W_c in ω space in this purely classical absorption model. Heller[6a] has obtained a similar result which he refers to as the reflection approximation.[6c]

B. The Quantum Picture. In contrast, the quantum mechanical expression for W tells us[4] that transitions will occur when $\hbar\omega = \epsilon_v^f - \epsilon_i^0$ with intensity $(2\pi/\hbar)|\langle X_i^0|\mu_{0f}|X_v^f\rangle|^2$. That is, the photon energy must match the rovibronic energy difference $\epsilon_v^f - \epsilon_i^0$, upon which the intensity is given by the usual[4] (Franck–Condon like) expression involving the square of the transition dipole's matrix element between X_i^0 and X_v^f. Notice that this quantum viewpoint involves knowledge of the final-state vibration rotation functions X_v^f, whereas the W_c picture involves knowledge of $E_f - E_0$ at geometries where $|X_i^0|^2$ is large.

(1) R. G. Gordon, *Adv. Mag. Reson.*, **3**, 1 (1968).

(2) E_0 and E_f are the initial- and final-state adiabatic electronic potential energy surfaces.

(3) It is indeed possible to develop a sequence of approximations which treat the noncommutation of h_e and T to higher order. For example, to first order in the commutator $[h_e,T]$

$$\exp\left[\frac{it}{\hbar}(h_e + T)\right] = \exp(ith_e/\hbar)\exp(iTt/\hbar)\exp\left(\frac{-i}{2}t[h_e,T]/\hbar\right)$$

The commutator $[h_e,T]$ involves the force exerted between the electronic and nuclear degrees of freedom. We have not pursued such extensions here becuase we feel that the purely classical treatment of T gives rise to most of the interesting behavior which we wish to treat. One of the earliest developments along these lines was made by M. Lax, *J. Chem. Phys.*, **30**, 1752 (1952). More recent work includes J. M. Schulman and W. S. Lee, *ibid.*, **74**, 4930 (1981); S-Y. Lee, *ibid.*, **76**, 3064 (1982); C. Noda and R. N. Zare, *J. Mol. Spectrosc.*, in press; M. Tamir, U. Halavee, and R. D. Levine, *Chem. Phys. Lett.*, **25**, 38 (1974).

(4) G. Herzberg, "Molecular Spectra and Molecular Structure", Vol. III, Van Nostrand-Reinhold, New York, 1966, Chapter II.

(5) L. D. Landau and E. M. Lifshitz, "Quantum Mechanics", Pergamon Press, Oxford, 1965, Chapter XI, pp 322–4.

(6) E. Heller has for several years been exploring connections between classical and quantum mechanical phenomena using the kind of ω-dependent correlation function employed here. See, for example, (a) E. J. Heller, *J. Chem. Phys.*, **68**, 2066 (1978); (b) *ibid.*, **68**, 3891 (1978), and references therein. (c) G. Herzberg, "Spectra of Diatomic Molecules", 2nd ed, Van Nostrand, Princeton, 1950, pp 391–4.

Both of the above interpretations have assumed the use of a monochromatic light source. In the event that the light source has "finite" frequency resolution (e.g., for a picosecond pulse, the Heisenberg frequency spread is $\sim 10^{12}$ s^{-1} or ~ 30 cm^{-1}), the ideas expressed above must be modified. In particular, the ω dependence of W or W_c must be multiplied by the ω-dependent *experimental* line shape function to obtain more proper interpretations. There are two other circumstances in which such finite frequency ranges need to be addressed: when the energy levels ϵ_v^f are broadened by "lifetime effects" (e.g., predissociation or intramolecular energy redistribution) and when the spacing between the ϵ_v^f ($\epsilon_v^f - \epsilon_{v\pm1}^f$) is small compared to the resolution ($\Delta\omega$) of the light source (e.g., in large molecules with many internal degrees of freedom). We will say more about these cases later.

C. Forced Correspondence between W and W_c. Clearly, the above interpretation of W is different from that of W_c. However, let us see what insight can be gained by considering situations[6] under which W is accurately approximated by W_c in the neighborhoods of the *true* quantum transition energies $\epsilon_v^f - \epsilon_i^0$. That is, "to what extent can the intensity pattern of W be adequately replicated by that of W_c near $\hbar\omega = \epsilon_v^f - \epsilon_i^0$?" From the quantum mechanical ω dependence of W we know the photon frequencies at which absorption will occur: $\hbar\omega = \epsilon_v^f - \epsilon_i^0$. In small-molecule spectroscopy and photochemistry these transition energies are often available from experiment. We can then ask at what (if any) molecular geometries *this* $\hbar\omega$ is equal to the partly classical electronic energy splitting, $E_f(\vec{R}) - E_0(\vec{R})$. That is, equating the quantum and partly classical expressions for the photon energy

$$\epsilon_v^f - \epsilon_i^0 \simeq E_f(\vec{R}) - E_0(\vec{R}) \tag{5}$$

allows us to determine those molecular geometries (if any) at which the electronic energy difference equals the *true* quantum energy difference. Let us denote geometries which satisfy this criterion by $\{\vec{R}_c\}$. It is, of course, possible that eq 5 is satisfied at *no* molecular geometry. In such cases, the partly classical rate expression predicts that light of that energy would not be absorbed. As we will see later, this amounts to saying that such events should have low (zero) intensity.

By also equating the partly classical intensity (at the above $\hbar\omega$) to the fully quantal intensity, we obtain what can be called the partly classical approximation to the Franck–Condon like intensity[4]

$$|\langle X_i^0|\mu_{0f}|X_v^f\rangle|^2 \simeq \sum_{\vec{R}_c} |X_i^0(\vec{R}_c)|^2 |\mu_{0f}(\vec{R}_c)|^2 \tag{6}$$

where the sum (or integral, if the set $\vec{R}_c$ is continuous) is over all molecular geometries which satisfy eq 5 for the given $\hbar\omega$. Equations 5 and 6 provide us with an approximate connection[6] between the quantum and partly classical expressions for the rates of photon absorption. Equation 6 is, of course, not exact. The left-hand side of eq 6 can vary rapidly with v (and hence $\hbar\omega$), and it is by no means obvious that the right-hand side will vary in exactly the same way with $\hbar\omega$ (through $\vec{R}_c$). The range of approximate validity of eq 6 can probably best be determined from experience.

Molecular geometries which satisfy eq 5 are special because they allow the classical (electronic) energy difference $E_f - E_0$ to equal the quantum (total) energy difference $\epsilon_v^f - \epsilon_i^0$. They are also special because, as we see from eq 5, the classical vibration–rotation kinetic energy is unchanged by the photon absorption at $\vec{R}_c$: $\epsilon_v^f - E_f(\vec{R}_c) = \epsilon_i^0 - E_0(\vec{R}_c)$. This fact will, as we show later, prove useful when we address how to use these partly classical ideas in classical trajectory studies of the time evolution of the molecule following photon absorption.

As mentioned earlier, any lack of precision in the light source's frequency should be incorporated into this forced correspondence by allowing ω to vary over the spectral line shape. As ω varies, a range of critical geometries $\{\vec{R}_c\}$ is sampled via eq 5 (with an additional multiplicative weighting factor equal to the spectral line shape function). Each member of this range of $\{\vec{R}_c\}$ values then contributes to the absorption intensity according to eq 6 but with the factor in eq 6 multiplied by the spectral line shape factor appropriate to each specific ω.

If there exists an uncertainty in the transition energies $\epsilon_v^f - \epsilon_i^0$ caused, for example, by a decay process involving the state ϵ_v^f, eq 5 and 6 must again be modified. The finite lifetime (τ_v^f) of the state ϵ_v^f gives rise to a Lorentzian absorption profile for transitions into ϵ_v^f. The Lorentzian's width ($\Gamma_v^f = (\tau_v^f)^{-1}\hbar$) is determined by the inverse of the decay lifetime. In such cases, ω must be allowed to vary over an interval $\hbar^{-1}(\epsilon_v^f - \Gamma_v^f) \lesssim \omega \lesssim \hbar^{-1}(\epsilon_v^f + \Gamma_v^f)$ which, through eq 5, again yields a range of $\{\vec{R}_c\}$ values each of which is used in eq 6 (multiplied by the Lorentzian intensity factor) to determine the absorption intensity.

D. Relevance to Specific Experimental Situations. Having considered the content of the quantal W and the classical W_c as well as the mechanism for simulating W by W_c near the quantum state energy differences, we can now address under what circumstances the quantal picture is preferable and when the partly or purely classical models are adequate or even more relevant. The various experimental situations considered will differ either in the characteristics of the light source (e.g., time resolution, frequency resolution) or in those of the energy levels of the absorbing molecules (e.g., metastable nature or vibrational state density).

1. Small and Large Molecule Limits. For small molecules in which the spacings between the levels ϵ_v^f can be resolved with the available light sources, the quantum state-specific formulation is certainly better; the entirely classical model does not even recognize the quantization of the levels ϵ_v^f. However, use of the quantum formulas in ab initio calculations requires knowledge of the final-state wave functions $\{X_v^f\}$. In contrast, the partly classical method, which employs state-specific energy differences $\epsilon_v^f - \epsilon_i^0$, requires knowledge of the potential energy surfaces $E_f - E_0$ only where $|X_i^0|^2$ is substantial. Hence, in situations where the $\{X_v^f\}$, which may span large regions of $\vec{R}$ space, are unknown, the partly classical picture is probably more useful for acutal calculations. In most absorption experiments, the molecule is initially in a low-energy vibrational state. Hence X_i^0 has most of its amplitude localized in regions of $\vec{R}$ space near the equilibrium geometry of the $E_0(\vec{R})$ surface.

For large molecules in which the spacings in $\{\epsilon_v^f\}$ are small compared to the light source's band width (which can still be quite narrow), fully state-specific quantal expressions become essentially useless. In many such cases, one wishes to focus attention on a small number of "active" internal degrees of freedom which are thought to play a central role in some dynamical process which follows absorption. For example, in the $n\pi^*$ photochemical decompostion of H_3CCOH to produce H_3CCO, the C–H "stretch" mode is certainly active; it is a dominant part of the reaction coordinate. The CO stretch coordinate is also probably active since the $n\pi^*$ electronic transition is likely to excite this vibration. On the other hand, the methyl group's vibrations and internal rotations are probably passive in the sense that they are not strongly involved in the reaction coordinate. In such cases, it is fruitful to treat the passive

modes as an energy reservoir characterized by a density of quantum states $\rho(\epsilon)$, and to assume that the coordinates of the reservoir degrees of freedom do not appear in μ_{0f}. The only role of the reservoir then is to provide a mechanism for the internal (vibration–rotation) excitation energy of the active modes to be redistributed into the modes of the reservoir. In effect, the reservoir allows each active-mode state ϵ_v^f to have a finite decay rate Γ_v^f which is assumed to be proportional to the number ρ of reservoir vibration–rotation states which have energy equal to $\epsilon_v^f - \epsilon_0^f$ (the amount of internal energy above the zero point of the E_f surface): $\Gamma_v^f \sim \rho(\epsilon_v^f - \epsilon_0^f)$. Because of the presence of this energy redistribution decay process, light of frequencies ω lying in the range $h^{-1}(\epsilon_v^f - \Gamma_v^f) \lesssim \omega \lesssim h^{-1}(\epsilon_v^f + \Gamma_v^f)$ (which may even overlap) can be absorbed, where the widths Γ_v^f increase with ϵ_v^f since $\rho(\epsilon_v^f - \epsilon_0^f)$ increases with ϵ_v^f. As ω varies, a range of $\{\vec{R}_c\}$ values are sampled (in the partly classical approach) via eq 5. These $\{\vec{R}_c\}$ values, when used in eq 6, weighted by the sum of the Lorentzian factors arising from each $(\epsilon_v^f,\Gamma_v^f)$ line, generate the partly classical approximation W_c appropriate to such large-molecule cases.

For small molecules whose final state energies ϵ_v^f are broadened by predissociative effects, the partly classical analysis outlined above for large molecules can still be applied. The primary difference in the two cases is that the intramolecular energy decay provides the width (Γ_v^f) in the large-molecule limit whereas predissociation causes the width in the other situation.

2. Dissociative States. There is one other reason for which ω must be allowed to vary continuously rather than to match a specified $\epsilon_v^f - \epsilon_i^0$. In the event that the final state $\phi_f X_v^f$ corresponds to dissociative motion along some direction, ϵ_v^f is certainly not quantized and X_v^f does not describe bound motion along this direction. In such cases (e.g., in direct photodissociation), the purely classical point of view, in which light of energy $\hbar\omega$ is absorbed whenever $\hbar\omega = E_f(\vec{R}) - E_0(\vec{R})$, is very relevant. In this picture, absorption occurs at all molecular geometries; the energy of the absorbed photon is *determined* from $\hbar\omega = E_f - E_0$ and the intensity of the absorption is proportional to $|\mu_{0f}(\vec{R})|^2$. The probability density for finding the molecule at $\vec{R}$ is $|X_i^0(\vec{R})|^2$. This then leads to the image relationship between the $\vec{R}$ dependence of $|\mu_{0f}|^2|X_i^0|^2$ and the ω dependence of W_c. For example, if $E_0(R)$ were well represented as a harmonic potential in one dimension (R), $E_0 = {}^1/_2kR^2$, and if $E_f(R)$ were, in regions where $|X_i^0|^2$ is large, accurately represented by an inverted and shifted (in energy by Δ) parabola, $E_f = \Delta - {}^1/_2\bar{k}R^2$, then the condition $\hbar\omega = E_f - E_0$ leads to $R_c^2 = 2(\Delta - \hbar\omega)/(k + \bar{k})$. If X_i^0 is taken to be of the form of the lowest energy harmonic oscillator function along R, $X_i^0 = A\exp(-\alpha R^2)$, then $|X_i^0|^2(R_c) = A^2\exp[-4\alpha(\hbar\omega - \Delta)/(k + \bar{k})]$, which presents the above-mentioned image relationship.

III. Relevance to Classical Trajectory Studies of Time Evolution

In addition to the insight into the nature of electronic transitions provided by the forced correspondence, we can make other uses of eq 5 and 6. Moreover, the fully quantum point of view and the classical point of view, both of which were shown above to have their own advantages, can be employed for more than understanding the absorption event. For example, we might wish to follow, by classical or semiclassical trajectory methods, the time development[6] of the state which is prepared by the absorption of a photon of energy $\hbar\omega$. To do so would be especially relevant if the state so prepared were subject to predissociation[7] (either by tunneling or by intramolecular energy transfer followed by bond rupture). We now turn our attention to the relevance of the above analysis of photon absorption intensities to such time evolution studies.

A. Time-Domain and Frequency-Domain Experiments. We first need to address how experimental measurements in either time or frequency space give information about the decay rates of molecules. Time-domain experiments use pulsed light sources, whose pulse duration is less than the lifetime τ of the decaying state. In this manner, one prepares the system in a nonstationary state which undergoes decay. The rate of decay can be monitored, for example, by monitoring the subsequent (after the initial pulse) fluorescence (direct or laser induced) of the *products* of the decay process. Such an approach forms the basis of so-called pump and probe techniques. It should be kept in mind that, in any such time-domain experiment, there exists a finite limiting frequency resolution caused by the Heisenberg uncertainty relation $\Delta\omega\,\Delta t \geq 1$. In experiments with short time pulses ($\Delta t \sim 10^{-12}$ s), the corresponding spread in photon frequency ($\Delta\omega \sim 10^{12}$ s^{-1})e can be rather large. To prepare the final state "before" it has time to decay, one must use a light source having a pulse duration less than the lifetime of the state. Hence the light source's frequency spread times $\hbar$ will be at least as large as the Heisenberg uncertainty in the final state's energy. The implications of such low-frequency resolution were discussed in sections II.B and II.C.

Within the domain of frequency-resolved spectroscopy, one can also infer these same decay rates. In producing a visible or UV light source of high-frequency resolution ($\Delta\omega \sim 10^9$ s^{-1}), one gives up the chance to use extremely short light pulses (since a pulse duration of $\Delta t \sim 10^{-9}$ s is considerably larger than isolated-molecule vibrational times). However, such light sources can still be used to probe processes which occur on short ($\sim 10^{-12}$ s) time scales. A decay process which occurs in τ s will cause a broadening (uncertainty) in the energy of the decaying state given by $\Delta E = \hbar\tau^{-1}$. Thus, as the (precisely known) frequency (ω) of the light source is scanned in a neighborhood ($\Delta\omega \sim \tau^{-1}$) of the decaying state, the state will be populated and undergo subsequent decay (on a time scale which may be much faster than the light source's duration). The decay rate of the final state can be inferred by measuring the frequency range $\Delta\omega$ (which can be done because the light source's frequency is precisely known) over which absorption takes place. The lifetime is then given by $\tau = \Delta\omega^{-1}$. Of course, this inference is only possible in the case where the dominant contribution to the absorption line width is the above decay process or where contributions from other sources can be removed.

B. Requirements of Classical Trajectory Investigations. To employ classical or semiclassical dynamics techniques to study such decaying states, one proceeds as follows:

(1) An ensemble of starting molecular geometries $\{\vec{R}_0\}$ and their corresponding momenta $\{\vec{P}_0\}$ are chosen. The ranges of $\vec{R}_0$ and $\vec{P}_0$ as well as the relative probabilities of

(7) If the state $\phi_f X_v^f$ is predissociative, the energy splittings $\epsilon_f^f - \epsilon_i^0$ are not rigorously defined because the state $\phi_f X_v^f$ has a finite lifetime τ_v^f which gives rise to a width ($\Gamma_v^f = \hbar/\tau_v^f$) in its energy. However, for reasonably long-lived states (i.e., where Γ_v^f is less than the spacing between neighboring ϵ_v^f levels), the experimental absorption spectrum retains sufficient structure to permit one to reasonably accurately estimate $\epsilon_v^f - \epsilon_i^0$ (and even Γ_v^f). If the state $\phi_f X_v^f$ is dissociative, then X_v^f will involve, along one of the molecule's internal degrees of freedom, an unbound or continuum wave function. The contribution to ϵ_v^f arising from this degree of freedom will not be quantized. In such cases, it is probably best to treat $\hbar\omega$ as varying continuously, and to then use $\hbar\omega = E_f(\vec{R}) - E_0(R)$ and eq 6 to find the "critical" geometries $\vec{R}_c$ and their corresponding (eq 6) intensities.

each such starting condition are determined so as to replicate the experimentally prepared state. More is said below about how this is achieved.

(2) For each starting geometry and momentum, the classical equations of motion (or their semiclassical generalizations) are integrated as functions of time.

(3) The eventual fate (e.g., dissociation into various internal states of the fragments) of each trajectory is recorded as is the time it takes the decay (e.g., dissociation) to occur. After the ensemble of trajectories has been so propagated, the distribution of decay times, product-species internal-state populations, etc. can be used to compute the averages of these properties. In this way, one can compute the average decay rate of the ensemble which is designed to replicate some experimentally prepared system.

C. Choosing Starting Coordinates and Momenta. The connection between our analysis of the photon-absorption process and such trajectory studies can now be made clearer. The distribution (range and probability) of starting geometries for the dynamics study of the decaying state is determined by the distribution of geometries at which photons are absorbed. Within the partly classical point of view outlined earlier, the $\vec{R}_c$ values are the appropriate starting geometries and $|\mu_{0f}|^2|X_i^0|^2$ is the probability weighting for each $\vec{R}_c$. Within the purely quantum picture, $|\langle\phi_f X_v^f|\vec{\epsilon}\cdot\vec{r}|\phi_0 X_i^0\rangle|^2|X_v^f(\vec{R})|^2$ gives the relative probability of each $\vec{R}$ value; $|\langle X_v^f|\mu_{0f}|X_i^0\rangle|^2$ giving the relative probability for arriving in X_v^f and $|X_v^f|^2$ giving the probability of being at $\vec{R}$ given that the molecule is in X_v^f.

(1) The Quantum Picture. To utilize the fully quantum state-resolved formula (eq 1) to determine starting momenta, we need to know the discrete energy level differences $\epsilon_v^f - \epsilon_i^0$ as well as the excited-state vibration–rotation wave functions X_v^f. The former ($\epsilon_v^f - \epsilon_i^0$) we can usually estimate from the molecule's absorption spectrum; the X_v^f are, however, often very difficult to estimate. Of course, in both the quantum and partly classical models, we need to know the electronic transition dipole[4] $\mu_{0f}(\vec{R})$. Given a value or range of values of $\epsilon_v^f - \epsilon_i^0 = \hbar\omega$, $|X_v^f|^2(\vec{R})$ then determines the probability density governing the molecule's nuclear coordinates. The molecule's momenta are then constrained to obey[8] $\epsilon_v^f - E_f(\vec{R}) = T_c(\vec{R})$. This simply states that the total energy ϵ_v^f minus the potential energy $E_f(\vec{R})$ equals the nuclear kinetic energy $T_c(\vec{R})$. For situations where there is some range of ω values absorbed, it is more useful to express (using $\hbar\omega + \epsilon_i^0 = \epsilon_v^f$) this result as $T_c = \hbar\omega + \epsilon_i^0 - E_f$. As ω varies, this then gives the corresponding range of T_c values. Classical trajectories which correspond to such initial $\vec{R}$ and $T_c(\vec{R})$ values can then be run and weighted by the probability ($|\langle X_v^f|\mu_{0f}|X_i^0\rangle|^2$) for producing $\phi_f X_v^f$ times the probability $|X_v^f(\vec{R})|^2$ of observing an initial $\vec{R}$ value *given* that the vibration–rotation wave function is X_v^f.

(2) *The Partly Classical and Classical Perspectives.* In contrast, the partly classical treatment of the trajectory problem requires knowledge of $\epsilon_v^f - \epsilon_i^0$ (from which (eq 5) possible $\vec{R}_c$ values[9] can evaluated), $|X_i^0(\vec{R}_c)|^2$, and, of course, $|\mu_{0f}(\vec{R}_c)|^2$. In comparison with the full quantal treatment, knowledge of $X_v^f(\vec{R})$ is replaced by knowledge of $X_i^0(\vec{R}_c)$. This represents a potential computational advantage of the partly classical approach because, as mentioned above, the excited-state vibration–rotation functions X_v^f are often difficult to approximate. Given the positions of the peaks in a molecular absorption spectrum (i.e., values of $\epsilon_v^f - \epsilon_i^0$), classical trajectories can be propagated by first determining the values[9] $\vec{R}_c$ at which $\epsilon_v^f - \epsilon_i^0 = E_f(\vec{R}_c) - E_0(\vec{R}_c)$. The probability weighting factor for such an initial $\vec{R}_c$ value is taken as $|X_i^0(\vec{R}_c)|^2|\mu_{0f}(\vec{R}_c)|^2$. Noticing that $\epsilon_v^f - E_f(\vec{R}_c) = \epsilon_i^0 - E_0(\vec{R}_c) = T_c$ states that the classical kinetic energy remains unchanged at these special $\{\vec{R}_c\}$ geometries, allows one to constrain the initial momenta at $\vec{R}_c$ to obey[8] $T_c(\vec{R}_c) = \epsilon_i^0 - E_0(\vec{R}_c)$. If $\hbar\omega$ is uncertain, due to finite ω resolution or the pulse time of the light source or to lifetime width in the ϵ_v^f energy level, a range of $\{\vec{R}_c\}$ and $\{T_c(\vec{R}_c)\}$ values results from allowing ω to vary. Each $\vec{R}_c$ and $T_c(\vec{R}_c)$ represents a valid point for starting classical of semiclassical trajectories.

The purely classical analysis goes through very much as above except that $\hbar\omega$ is no longer restricted to equal $\epsilon_v^f - \epsilon_i^0$. Rather any photon energy is acceptable; $\hbar\omega = E_f - E_0$ then determines the $\vec{R}_c$, eq 6 gives the probability weighting of this $\vec{R}_c$, and $T_c = \epsilon_i^0 - E_0(\vec{R}_c)$ constrains the momenta.

(3) More on Starting Momenta. The conservation of kinetic energy condition $T_c = \epsilon_i^0 - E_0(\vec{R}_c) = \epsilon_v^f - E_f(\vec{R}_c)$ which arises in the partly classical picture needs to be clarified. For molecules with only one internal degree of freedom (or only one active mode), the above identity is enough to *determine* the momentum values corresponding to $\vec{R}_c$. For example, if $E_0(R)$ is a one-dimensional diatomic potential, $T_c = P_c^2/2\mu = \epsilon_i^0 - E_0(R_c)$ can be solved for the two P_c values $P_c = \pm[2\mu(\epsilon_i^0 - E_0(R_c))]^{1/2}$ which are consistent with any R_c. However, when $E_0(\vec{R})$ depends upon more than one internal degree of freedom, the situation is more complicated.

If, in regions where $|X_i^0|^2$ is significant, the "shape" of $E_0(\vec{R})$ is such that the molecule's vibration–rotation motion is mode separable, then ϵ_i^0 reduces to a sum of energies for each active mode: $\epsilon_i^0 = \sum_n \epsilon_{in}^0$. Consistent with this separability is the *local* (where $|X_i^0|^2$ is large) separability of E_0: $E_0(\vec{R}) = \sum_n E_{0n}(\vec{R}_n)$. In such cases, the molecule vibrates indeependently along each mode direction and hence it is possible to say that, along each mode direction $\vec{R}_n$, $T_{cn}(\vec{R}_{cn}) = \epsilon_{in}^0 - E_{0n}^0(\vec{R}_{cn})$ where $\vec{R}_{cn}$ is the coordinate of $\vec{R}_c$ along this nth mode. Hence, we can actually determine the momentum (to within a sign along each mode (i.e., $P_{cn}^2/2\mu_n = \epsilon_{in}^0 - E_{0n}(\vec{R}_{cn})$) in this separable case. These momenta can then be used, together with the $\vec{R}_{cn}$, as initial values for trajectories.

For systems in which the modes are so strongly coupled that such a separation is impossible, one has a more difficult task. It is possible, for a given total energy ϵ_i^0, to follow a huge number of classical trajectories whose starting spatial distribution is $|X_i^0(\vec{R})|^2$ and to tabulate the values of $\vec{P}$ (along all internal coordinates) which occur at geometries $\vec{R}_c$ obeying $\epsilon_v^f - \epsilon_i^0 = E_f(\vec{R}_c) - E_0(\vec{R}_c)$. In this way, we could associate with any $\vec{R}_c$ a set of $\vec{P}$ values which are consistent with the condition $T_c(\vec{R}_c) = \epsilon_i^0 - E_0(\vec{R}_c)$.

Alternatively, one can compute the Wigner phase space function $^{10}\Gamma(\vec{R},\vec{P})$ belonging to the spatial wave function $X_i^0(\vec{R})$. This function gives the probability density for observing an initial coordinate $\vec{R}$ and an initial momentum $\vec{P}$, given that the system's wave function is $X_i^0(\vec{R})$. Because of the kinetic energy conservation condition discussed

(8) The single constraint does not, of course, *determine* the molecule's nuclear momenta except when there is only one nuclear motion degree of freedom (when $\epsilon_v^f - E_f(\vec{R}) = p^2/2\mu$). For a molecule with N internal degrees of freedom, the condition $\epsilon_v^f - E_f(\vec{R}) = T_c$ provides a constraint that allows one to choose $N-1$ internal momenta (as initial conditions) from which the Nth momentum can be evaluated.

(9) For multidimensional potential energy surfaces, the condition $E_f(\vec{R}_c) - E_0(\vec{R}_c) = \epsilon_v^f - \epsilon_i^0 = \hbar\omega$ can be obeyed at an infinite number of $\vec{R}_c$ values. Each of these $\vec{R}_c$ values represents an acceptable initial condition for use in a classical trajectory calculation.

(10) R. C. *Brown* and E. J. Heller, *J. Chem. Phys.*, **75**, 186, 1048 (1981).

above, one can use these same Wigner momentum densities together with the Wigner $\vec{R}$ space densities at the critical $\vec{R}_c$ values to describe initial conditions for propagating trajectories on the excited surface.

To implement the Wigner distribution method for computing probability weighting factors for initial momenta, we could proceed as follows. Given a value of $\hbar\omega$ which obeys $\hbar\omega = \epsilon_{v'}{}^f - \epsilon_v{}^0$, one searches for geometries $\vec{R}_c$ at which $\hbar\omega = E_f - E_0$. At each such geometry $\Gamma(\vec{R}_c,\vec{P})$ gives the probability weighting to assign to $\vec{R}_c,\vec{P}$. However, not all of the momenta $\{\vec{P}\}$ are independent. They must be constrained to obey the kinetic energy conservation condition $T(\vec{R}_c) = \sum_{i=1}^{N}(P_i^2/2\mu_i) = \epsilon_i^0 - E_0(\vec{R}_c)$. Hence, in sampling the momentum space, one need only choose $N-1$ initial momenta; the Nth momentum is determined.

For example, if one is dealing with a triatomic molecule in which only the two stretching degrees of freedom (x,y) are "active" the Wigner function $\Gamma(x,y,p_x,p_y)$ is (in a harmonic approximation)

$$\Gamma = \frac{(-1)^{v_x+v_y}}{(\pi h)^2} L_{v_x}{}^0\left(\frac{2\mu_x\omega_x}{h}x2 + \frac{2}{\mu_x\omega_x h}p_x{}^2\right) L_{v_y}{}^0\left(\frac{2\mu_y\omega_y}{h}y^2 + \frac{2}{\mu_y\omega_y h}p_y{}^2\right) \exp\left[-\frac{\mu_x\omega_x}{h}x^2 - \frac{p_x{}^2}{\mu_x\omega_x h} - \frac{\mu_y\omega_y}{h}y^2 - \frac{p_y{}^2}{\mu_y\omega_y h}\right]$$

Here $\mu_{x,y}$, $\omega_{x,y}$, and $v_{x,y}$ are the reduced masses, vibrational frequencies, and quantum numbers of the two degrees of freedom. $L_v{}^0$ is the vth Laguerre polynomial. The kinetic energy conservation statement $E_i^0 - E_0(\vec{R}_c) = p_x{}^2/2\mu_x + p_y{}^2/2\mu_v$ allows either p_x or p_y to be eliminated. As a result, Γ depends only on $\vec{R}_c = x_c,y_c$ and one of p_x and p_y. For any choice of $\hbar\omega$, $E_f(\vec{R}_c) - E_0(\vec{R}_c) = \hbar\omega$ then determines a set of $\vec{R}_c$ values, the weighting of each is being obtained from Γ. Choosing, for example, p_x, determining p_y from the kinetic energy condition, and obtaining the weighting of p_x,p_y from Γ then completes the determination of the initial conditions and the corresponding probabilities.

Operationally, there is a more efficient way to implement the above outlined procedures. By *first* sampling (via a grid chosen to span regions of x,y space where $X_v{}^0(x,y)$ is significant) values of x and y one can use $E_f(\vec{R}) - E_0(\vec{R}) = \hbar\omega$ to *infer* the value of ω at which this geometry will absorb light. Choosing, for example, p_x and determining p_y from kinetic energy conservation allows one to assign a probability weighting to this specific (x,y,p_x,p_y,ω) starting condition. Propagation of this trajectory leads to some outcome (e.g., dissociation after some time τ). This outcome (τ) therfore can be associated with absorption of light of energy $\hbar\omega$ determined as described above. If desired, each such ω value can be asssigned to a state-specific quantum transition $\epsilon_v{}^0 \rightarrow \epsilon_{v'}{}^f$ by standard histogram techniques (i.e., by assigning the lifetime τ and frequency ω to the transition $\epsilon_v{}^0 \rightarrow \epsilon_{v'}{}^f$ for which $\hbar\omega \equiv \epsilon_{v'}{}^f - \epsilon_v{}^0$ is most closely obeyed).

In utilizing the fully quantum approach[11] for computing initial coordinates and momenta, one is faced with a somewhat more severe difficulty. As discussed above, the $|\langle X_i^0|\mu_{0f}|X_v{}^f\rangle|^2$ values give the relative probabilities of being in the $\phi_f X_v{}^f$ states. $|X_v{}^f|^2$ then gives the $\vec{R}$ space probability density for any f state $\phi_f X_v{}^f$. The momenta are then constrained to obey (for any $\vec{R}$) $T_c(\vec{R}) = \epsilon_v{}^f - E_f(\vec{R})$. Even if $\epsilon_v{}^f$ and $E_f(\vec{R})$ are mode separable ($\epsilon_v{}^f = \sum_n \epsilon_{vn}{}^f$, $E_f = \sum_n E_{fn}(\vec{R}_n)$), one has to know E_f and $X_v{}^f$ for *all* regions of $\vec{R}$ space where $|X_v{}^f|^2$ is substantial. Moreover, it is less likely that E_f (and thus $\epsilon_v{}^f$) will be mode separable for such wide regions of $\vec{R}$ space. Of course, this discussion is predicated upon the assumption that X_i^0 is a low-energy state of E_0 whereas the $X_v{}^f$ span low-, intermediate-, and high-energy states of E_f. Such is, however, usually the case in experiments which start in the stable molecule at room temperature (for which X_i^0 is a low-energy vibrational–rotationl function) and produce an electronically excited species. Although the quantum approach suffers from the above difficulty, it has been successfully employed by ourselves[12] as a device for selecting starting coordinates and momenta for use in classical trajectory computations.

IV. Summary

In this paper we attempted to explore relationships among the quantum, classical, and partly classical views of photon-induced electronic transitions in molecules. We also discussed effects in the electronic absorption spectrum caused by finite frequency or time resolution of the exciting light source or by lifetime (intramolecular or predissociative) broadening of the molecule's excited states. The special relevance of the quantal and partly classical approaches to each of these situations was also explored. Finally, we demonstrated the relevance of our analysis of the photon absorption event to the problem of choosing starting molecular coordinates and momenta for use in classical trajectory studies of the molecule's behavior after photon absorption. Throughout the paper, emphasis was placed on conceptual matters as well as those dealing with the computational implementation of the working equations.

Acknowledgment. I acknowledge helpful communication with Professors E. Heller, W. Fink, and A. Banerjee concerning this work. Acknowledgment is made to the donors of the Petroleum Research Fund, administered by the American Chemical Society, for the support of this research.

(11) By fully quantum we do not, of course, refer to how the postabsorption dynamics is treated. We simply mean that quantum energies $\epsilon_v{}^f$ and wave functions $X_v{}^f$ are used.

(12) D. T. Chuljian, J. Ozment, and J. Simons, *Int. J. Quantum Chem.*, in press.